EXPERIMENTAL STUDY OF THE CUTTING RESULTANT FORCE FROM THE ALUMINIUM ALLOY TURNING PROCESS EN AW 6082

Claudiu Mihai NEDEZKI [1], Adrian TRIF [2] , Florin BUGNAR

ABSTRACT: The alloy EN AW 6082 (cylindrical) has undergone the turning process under different cutting regimes (cutting depth t, feed rate f, cutting speed v) while the forces that appear in the process were measured every time with the DKM 2000 dynamometer. On the other hand, the Kienzle model for calculating forces was also used. The novelty consists of the way the model coefficients were calculated (*p, f, r* respectively $k_{p1,1}$, $k_{f1,1}$, $k_{r1,1}$) – as a ***gradient of the line***, respectively the ***origin ordinate*** of the double logarithmic representation of the dependency between ***the specific force and the thickness of the unbroken chip (log Kp - log a).*** The ***measured values*** were compared to ***the ones calculated*** from the cutting forces. All calculations have been made in ***Excel,*** which helped to create the diagrams that express the influence of the cutting regime on the cutting process forces. Diagram interpretation led to the establishment of several important conclusions regarding the cutting process of the aluminium alloy.

KEY WORDS: the Kienzle model, model coefficients, slope, origin ordinate, dynamometer.

1 THEORETICAL CONSIDERATIONS

In the cutting process, the tool exerts a force F_R over the workpiece, on the strength of which the added processing material is deformed and removed as a chip, while defying all shearing and friction resistances. According to the mechanics laws, at the same time, on the workpiece appears a a force F_R' (the reaction force of the F_R force), which is called cutting force. Therefore, for the cutting process to happen, the work done by the lathe has to be higher than the resistant work done, afferent to all the shearing and friction resistances, meaning: $L_{MU} > L_R$.

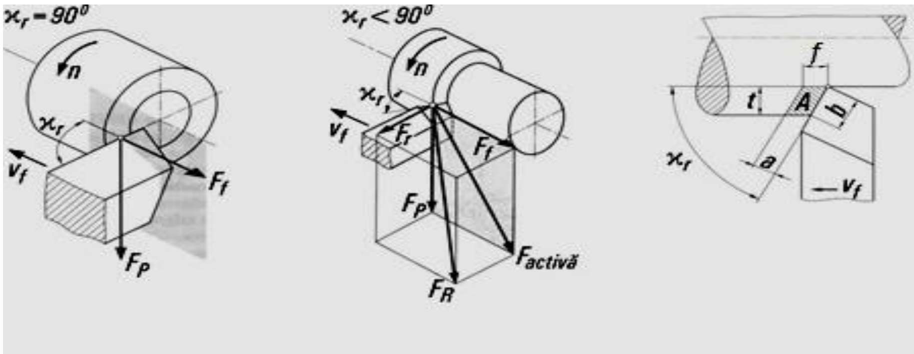

Technological parameters: t - depth of cut; f – feed rate
Geometrical parameters: a - thickness of the unbroken chip; b – widt of the unbroken chip
Area of the unbroken chip: a·b = t·f

Fig.1 The components of the cutting resultant force in the case of longitudinal turning and the unbroken chip section

The cutting resultant force F_R that appears in the turning process can be decomposed following the directions of a tridimensional system with the origin in a point of the cutting edge of the tool while the axes are oriented after the cutting movement direction, feed movement and the generated normal direction. The components of the cutting resultant force that are oriented after these directions are:

- ***The main component F_P*** , which represents the force that is necessary for overcoming the cutting resistance that occurs on the direction of the cutting movement. This

[1] Technical University of Cluj-Napoca; e-mail: Claudiu.Nedezki@muri.utcluj.ro
[2] Technical University of Cluj-Napoca; e-mail: adrian.trif@tcm.utcluj.ro

- component consists of the force that the added processing material presses on the rake face of the tool, determining the resistance torque on the main axe of the tool.
- ***The feed component*** F_f, is the force which is necessary for overcoming the cutting resistance that occurs on the direction of the cutting movement, resistance which opposes the penetration of the tool in the added processing material. This component mainly solicits the elements of lathe's feed mechanism.
- ***The passive component (of rejection)*** F_r, represents the force that is necessary for overcoming the cutting resistance on the generated direction of the normal, having the tendency to reject the cutting edge of the material layer to be cut, becoming an important source of dimensional deviations.

The components F_P, F_f, F_r are used for both calculations for sizing cutting tools and main elements of the tools and pieces fixing devices and for mechanisms sizing and lathe driving.

The size of the resultant force (implicitly of its components) is determined by the complex of factors that generally influence any cutting process, which are:

- the workpiece material and its technological and mechanical properties;
- cutting tool's material, geometry and the wear degree;
- cutting regime's parameters (cutting depth t, feed rate f, cutting speed v);

the cutting environment.

2 THE KIENZLE MODEL

This model is used for analytical modeling of resulting cutting force components from turning. The KIENZLE MODEL is based on the hypothesis that the decisive elements in the calculation of the resultant cutting force components are:

- technological parameters of the unbroken chip section (t - depth of cut; f – feed rate)

specific cutting force in the direction of the respective component (K_p, K_f, K_r)

$$\begin{cases} F_P = K_P \cdot t \cdot s \\ F_f = K_f \cdot t \cdot s \\ F_r = K_r \cdot t \cdot s \end{cases} \Leftrightarrow \begin{cases} F_P = K_P \cdot A \\ F_f = K_f \cdot A \\ F_r = K_r \cdot A \end{cases} \Leftrightarrow \begin{cases} F_P = K_P \cdot a \cdot b \\ F_f = K_f \cdot a \cdot b \\ F_r = K_r \cdot a \cdot b \end{cases} \quad (1)$$

The specific cutting force (***K_P, K_f, or K_r***) is the cutting component related to the surface of the unbroken chip. reprezintă componenta de aşchiere raportată la suprafaţa secţiunii aşchiei nedetaşate.

This size is characteristic of processed material (due to its specific resistance to cutting process) and depends significantly on thickness of the unbroken chip.

$$K_P = \frac{F_P}{A} = C_p \cdot a^{-p}; \qquad K_f = \frac{F_f}{A} = C_f \cdot a^{-f}; \qquad K_r = \frac{F_r}{A} = C_r \cdot a^{-r} \quad (2)$$

In case of a chip section having unitary geometric parameters (*a = 1, b = 1,* $\rightarrow$ *A = 1 mm²*), the constants C_p, C_f, C_r receive the notations $k_{p1,1}$, $k_{f1,1}$, $k_{r1,1}$ respectively and the name of the ***main value of the specific force***.

$$K_P = k_{p1,1} \cdot a^{-p}; \qquad K_f = k_{f1,1} \cdot a^{-f}; \qquad K_r = k_{r1,1} \cdot a^{-r} \quad (3)$$

By applying the logarithms, equation (3) is linearized:

$$\begin{aligned} \log K_P &= \log k_{p1,1} - p \cdot \log a; \\ \log K_f &= \log k_{f1,1} - f \cdot \log a; \qquad (4) \\ \log K_r &= \log k_{r1,1} - r \cdot \log a \end{aligned}$$

In the relations (4) as equations of the straight lines in double logarithmic coordinates **(logK_P - log*a*, logK_f - log*a*, logK_r - log*a*)**, it is observed that the coefficients ***p, f, r,*** represent the gradient of the straight lines and **log $k_{p1,1}$, log $k_{p1,1}$, log $k_{p1,1}$** represent the origin ordinate of the lines (4). Therefore, if known 2 points on the straight line in double logarithmic coordinates (4) can easily determine the coefficients of the model, as in the examples of Figure 2.

In Figure 2 (a and b) it shows the dependence of *the specific cutting force* KP on the thickness of the unbroken chip (both in the linear coordinate system and the double-logarithmic), for turning a cylindrical steel workpiece (33MoCr11), with the carbide insert (P10) at a cutting speed of 100 m / min, the insert having the following geometry: $\alpha = 5^0$, $\gamma = 6^0$, $\chi_r = 60^0$, $\lambda_T = 4^0$, $r_\varepsilon = 0{,}5$ mm

= f (a) in the different decimal areas of thickness of the chip

The exponent p is the gradient of the straight line KP = f (a) in double logarithmic representation and ***log*** $\boldsymbol{k_{p1,1}}$ is the origin ordinate of this straight line.

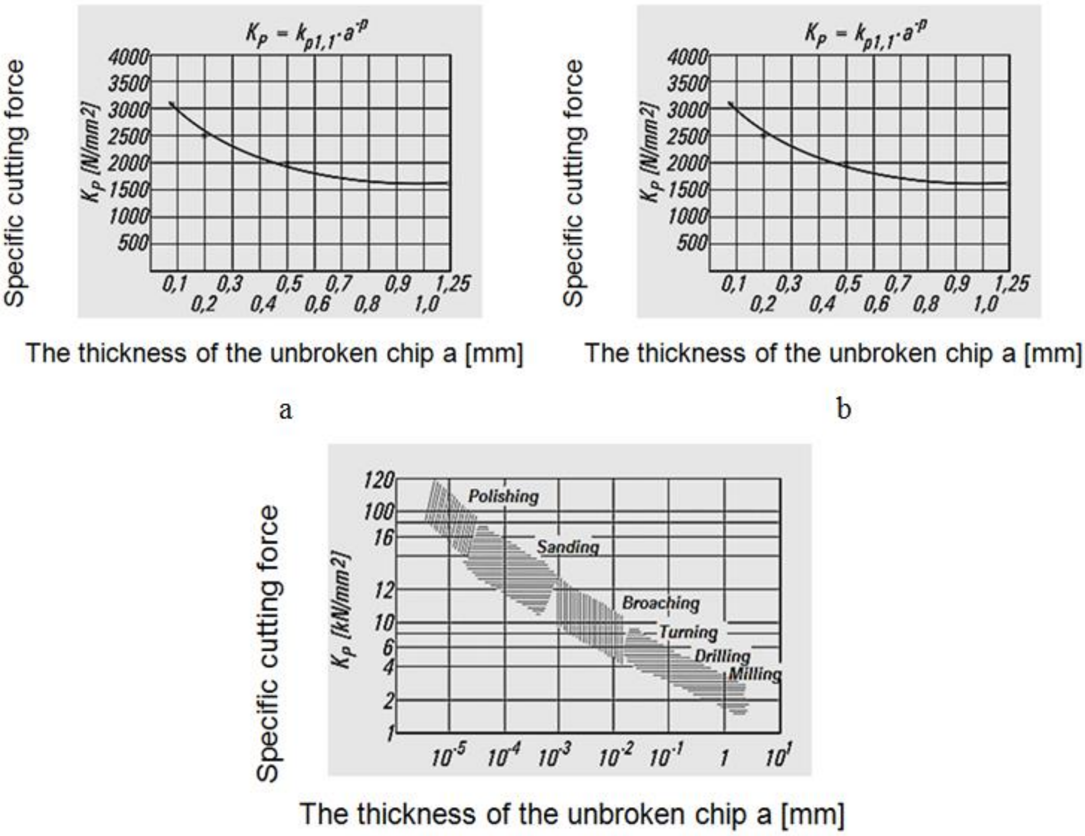

Fig.2 a,b,c. The dependence of the specific force on thickness of the unbroken chip (in linear an double logarithmic system) and the dependence K_P

$$p = \tan\Omega = \frac{DB}{AB} = \frac{\log 2250 - \log 1700}{\log 1 - \log 0{,}315} = \frac{\log\left(2250/1700\right)}{\log\left(1/0{,}315\right)} = \frac{0{,}121733596}{0{,}501689446} = 0{,}242647312 \qquad (5)$$

From specialized literature it is known that each cutting process (sanding, broaching, turning, milling, etc. - Figure 2c) corresponds to a particular decimal area of thickness of the unbroken chip, each of them corresponding a specific average of specific force KP and a specific amount of its increase ***(1- p)***.

Considering the expression of specific force (3), the resultant cutting force components are expressed by geometric parameters of section of the unbroken chip with following relations (6)

The resultant cutting force components are expressed by technological parameters of section of the unbroken chip and by the cutting edge angle of attack of the tool χ_r, with following relationships:

$$F_P = k_{p1,1} \cdot b \cdot a^{1-p}; \qquad F_f = k_{f1,1} \cdot b \cdot a^{1-f}; \qquad F_r = k_{r1,1} \cdot b \cdot a^{1-r} \qquad (6)$$

$$F_P = k_{p1,1} \cdot t \cdot s^{1-p} \cdot \sin^{-p} \chi_r; \quad F_f = k_{f1,1} \cdot t \cdot s^{1-f} \cdot \sin^{-f} \chi_r; \quad F_r = k_{r1,1} \cdot t \cdot s^{1-r} \cdot \sin^{-r} \chi_r \qquad (7)$$

3 EXPERIMENTAL RESEARCH

The composition of EN AW 6082 alloy are presented in Table 1

The EN AW 6082 alloy is successfully used as high load structures for frames of trucks or buses, for boiler or bicycle, for boat construction, for hydraulic systems, flanges, drilling equipment, poles, towers, speedboats, masts, metal scaffolding, frames for tents.

Table 1

Si	Fe	Cu	Mn	Mg	Cr	Zn	Ti	Other	Al
0.7-1.3	<=0.5	<=0.10	0.4-1.0	0.6-1.2	<=0.255	<=0.20	<=0.10	0.05	Rest
The values are expressed in %									

From this material can perform a huge variety of industrial profiles (round bars, rectangular bars, drawn or extruded bars, profiles, boards, etc.) profiles that meet the most stringent European quality standards, to provide high performance for optimal use. The **EN AW 6082** bars have a wide applicability in the field of machine constructions as well as welded constructions. Perfectly matches the requirements needed to prepare parts / components subject to requests oscillating, rotating parts, being used as motherboards of different subassemblies. Can be made from this alloy housings for hydraulic pumps or parts of hydraulic systems.

4 THE EXPERIMENT

Experimental conditions:

Machine: SNA 560x1000 universal normal lathe

Cutting environment: dry cutting

Cutting tool: straight knife with carbide insert (P20 quality)

The geometry of the cutting tool:

$$\alpha_O = 6^0; \quad \gamma_O = 6^0; \quad \lambda_T = 0^0; \quad \chi_r = 90^0$$

$$\textit{respectively } 45^0; 60^0; 75^0; 90^0 \textit{ to } 17-20$$

$$\exp\textit{eriment};$$

$$\chi_r^{'} = 30^0; \quad r_\varepsilon = 0{,}5\, mm$$

The workpiece: aluminum bar EN AW 6082

The dynamometer with resistive transducer (DKM 2010): The dynamometer (Figure 3) allows the measurement of the three components - through the resistive electrical transducers, - having a system for data acquisition and processing on the computer through a software designed for this purpose ([1],[2],[3]). The operating principle of the dynamometer is shown in Figure 3 and the instructions for use (together with the related software - XKM 2000) in ([4])

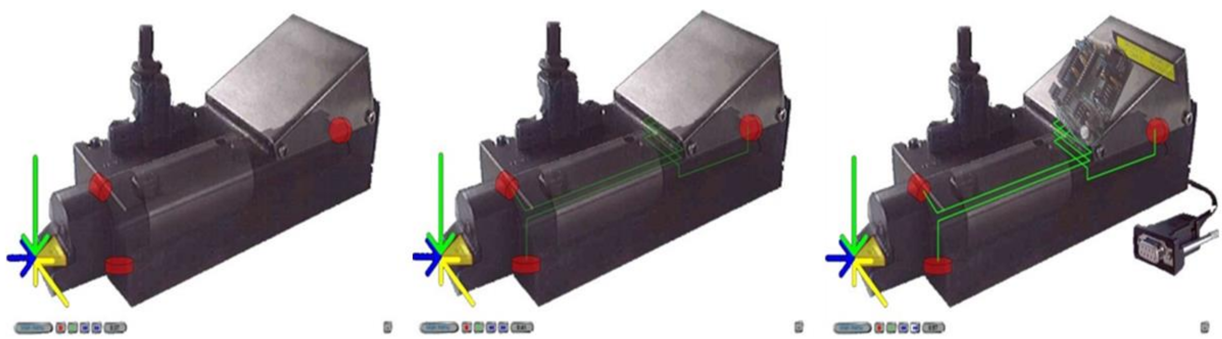

Fig.3 The operating principle of dynamometer for turning DKM 2010 (BAGS laboratory equipment)

The dynamometers with resistive transducers have high performances: sensitivity, precision, convenience in testing, simple equipment, etc. The principle is to mount in series with the force to be measured of a elastic element that may have stuck the resistive transducers. The elastic element must have a rigidity as high as possible in relation to the sensitivity of the transducer which will measure the deformation under the action of the force in question.

Summarizing table with experimental data are shown below:

Table 2

Nr. crt.	D [mm]	n [rot/min]	v [m/min]	t [mm]	f [mm/rot]	χ [°]	a [mm]	b [mm]	A [mm²]	$F_{P,măs}$ [N]	$F_{f,măs}$ [N]	$F_{r,măs}$ [N]	K_P [N/mm²]	K_f [N/mm²]	K_r [N/mm²]	log a	log K_P	log K_f	log K_r	$F_{P,calc}$ [N]	$F_{f,calc}$ [N]	$F_{r,calc}$ [N]
1			67,25	0,5			0,2	0,5	0,1	*208*	*103*	*51*	4100	2010	1710	-0,698	3,612	3,303	3,232	191,11	93,62	36,75
2			67,25	0,75			0,2	0,75	0,15	*317*	*186*	*76*	4113,3	2360	1526,6	-0,698	3,614	3,372	3,183	286,6	140,43	55,12
3			67,25	1			0,2	1	0,2	*431*	*212*	*87*	3655	2275	1245	-0,698	3,562	3,356	3,095	382,22	187,24	73,27
4	68	315	67,25	1,5	0,2	90	0,2	1	0,2	*687*	*343*	*167*	4935	3215	1310	-0,698	3,693	3,507	3,117	573,33	280,87	110,25
5			68,24		0,1		0,1	1	0,1	*240*	*100*	*58*	1350	760	580	-1	3,13	2,88	2,763	215,33	97,87	56,94
6			68,24		0,2		0,2	1	0,2	*379*	*212*	*78*	1545	1060	350	-0,698	3,188	3,025	2,544	383,22	187,24	73,55
7			68,24		0,315		0,315	1	0,315	*578*	*318*	*90*	1330,1	1009,5	234,9	-0,501	3,123	3,004	2,37	546,39	286,83	86,27
8			68,24		0,4		0,4	1	0,4	*687*	*411*	*102*	1295	1077,5	255	-0,397	3,112	3,032	2,406	658,12	359,17	93,81
9			68,24		0,63	90	0,63	1	0,63	*986*	*580*	*112*	1046	920,6	177,7	-0,2	3,019	2,964	2,249	938,06	551,53	110,03
10	69	315	68,24	1	0,8		0,8	1	0,8	*1275*	*732*	*120*	852,5	863,7	150	-0,096	2,93	2,936	2,176	1130,52	689,41	119,66
11		200	42,07				0,2	0,5	0,1	*395*	*290*	*130*	3950	2900	1300	-0,698	3,596	3,462	3,113	191,11	93,62	36,77
12		315	66,26				0,2	0,5	0,1	*325*	*220*	*100*	3250	2200	1000	-0,698	3,511	3,342	3	191,11	93,62	36,77
13		400	84,15				0,2	0,5	0,1	*320*	*215*	*96*	3200	2150	960	-0,698	3,505	3,332	2,982	191,11	93,62	36,77
14		500	105,19				0,2	0,5	0,1	*305*	*201*	*87*	3050	2010	870	-0,698	3,484	3,303	2,939	191,11	93,62	36,77
15		630	132,53				0,2	0,5	0,1	*288*	*181*	*73*	2880	1810	730	-0,698	3,459	3,257	2,863	191,11	93,62	36,77
16	67	800	168,3	0,5	0,2	90	0,2	0,5	0,1	*273*	*163*	*59*	2730	1630	590	-0,698	3,136	3,212	2,77	191,11	93,62	36,77
17			66,26			45	0,14	0,5	0,707	*345*	*81*	*66*	487,97	114,56	437,05	-0,853	2,688	2,059	2,64	207,08	95,64	41,52
18			66,26			60	0,17	0,5	0,085	*323*	*95*	*53*	3800	1117,6	3094,11	-0,769	3,579	3,048	3,49	198,09	94,49	38,68
19			66,26			75	0,19	0,5	0,095	*315*	*101*	*46*	3315,7	1063,1	2642,1	-0,721	3,52	3,026	3,421	193,3	93,92	37,23
20	67	315	66,26	0,5	0,2	90	0,2	0,5	0,1	*325*	*113*	*35*	3250	1130	2350	-0,698	3,511	3,053	3,371	191,11	93,62	36,75

The calculation relationships used to completing the experimental table are shown schematically below:

The cutting speed:

$$v = \frac{\pi \cdot D \cdot n}{1000} \quad [m/\min]; \tag{8}$$

Geometrical parameters of the e unbroken chip

$$a = s \cdot \sin \chi_r; \quad b = \frac{t}{\sin \chi_r} \tag{9}$$

The section of the unbroken chip:

$$A = a \cdot b = t \cdot s \tag{10}$$

The specific cutting forces:

$$K_P = \frac{F_{P,mas}}{A}; \; K_f = \frac{F_{f,mas}}{A}; \; K_r = \frac{F_{r,mas}}{A}; \tag{11}$$

The coefficients (parameters) of the model is calculated from the expression of specific force:

$$p = \tan \Omega = \left| \frac{\log K_P(10) - \log K_P(5)}{\log a(10) - \log a(5)} \right| \tag{12}$$

signifies the gradient of the line

and

$\log k_{p1,1}$ signifies the origin ordinate

Free term of the line equation that passes through points (10) and (5) is $\log k_{p1,1}$:

$$\frac{\log K_P - \log K_P(5)}{\log K_P(10) - \log K_P(5)} = \frac{\log a - \log a(5)}{\log a(10) - \log a(5)} \tag{13}$$

Similary are calculated the coefficients:

$$\begin{cases} f = \left| \dfrac{\log K_f(10) - \log K_f(5)}{\log a(10) - \log a(5)} \right| \\ \log k_{f1,1} \; \textit{as origin ordinate of the line}: \\ \dfrac{\log K_f - \log K_f(5)}{\log K_f(10) - \log K_f(5)} = \dfrac{\log a - \log a(5)}{\log a(10) - \log a(5)} \end{cases} \tag{14}$$

$$\begin{cases} r = \left| \dfrac{\log K_r(10) - \log K_r(5)}{\log a(10) - \log a(5)} \right| \\ \log k_{r1,1} \textit{ as origin ordinate of the line}: \\ \dfrac{\log K_r - \log K_r(5)}{\log K_r(10) - \log K_r(5)} = \dfrac{\log a - \log a(5)}{\log a(10) - \log a(5)} \end{cases} \quad (15)$$

The components of the resultant cutting force:

$$F_P = k_{p1,1} \cdot t \cdot s^{1-p} \cdot (\sin \chi_r)^{-p};$$
$$F_f = k_{f1,1} \cdot t \cdot s^{1-f} \cdot (\sin \chi_r)^{-f}; \quad (16)$$
$$F_r = k_{r1,1} \cdot t \cdot s^{1-r} \cdot (\sin \chi_r)^{-r}$$

5 DIAGRAMS AND CONCLUSIONS

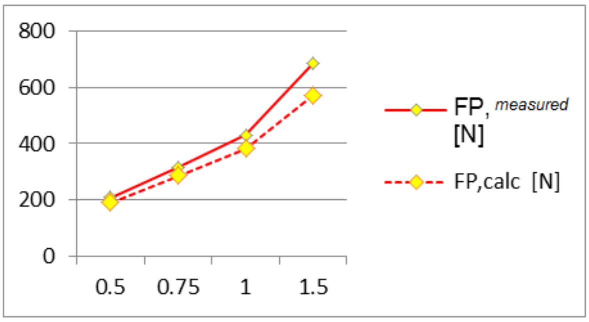

Fig. 4a The graph F_P = *f(f[mm/rev])*

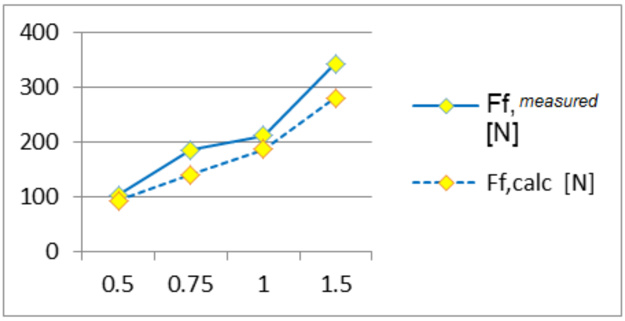

Fig.4b The graph F_f = *f(f[mm/rev])*

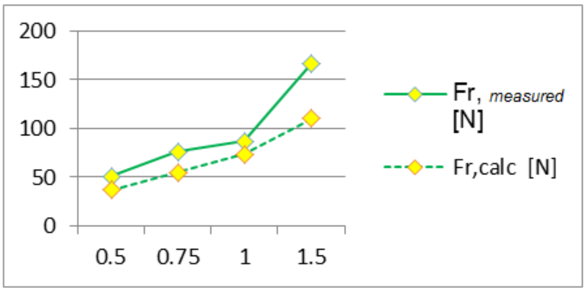

Fig. 4c The graph F_r = *f(f[mm/rev])*

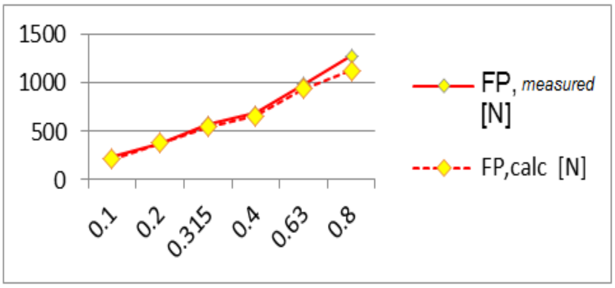

Fig. 4d The graph F_P = *f(t[mm])*

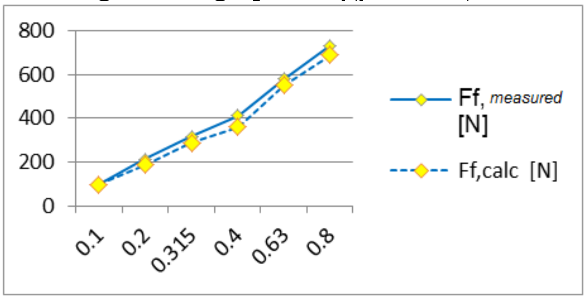

Fig. 4e The graph F_f = *f(t[mm])*

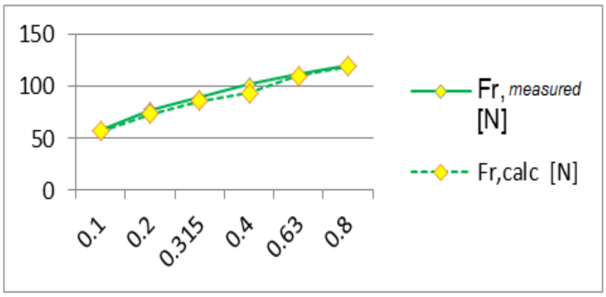

Fig. 4f The graph F_r = *f(t[mm])*

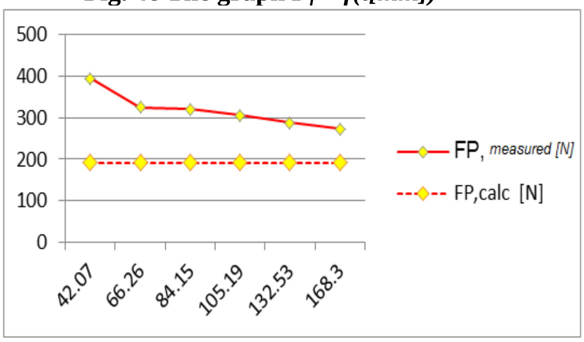

Fig. 4g The graph F_P = *f(v[m/min])*

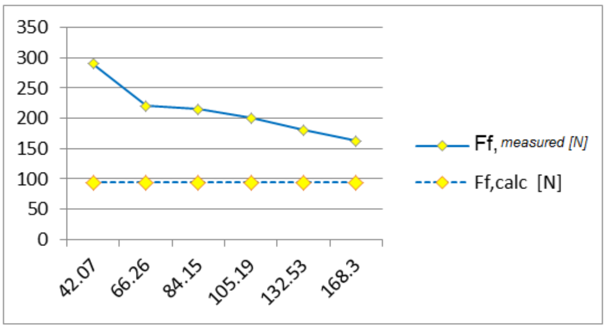

Fig. 4h The graph F_f = *f(v[m/min])*

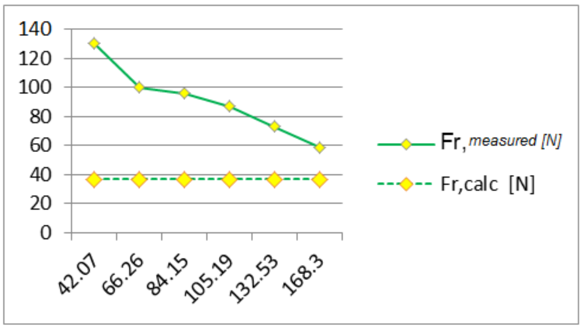

Fig. 4i The graph $F_r = f(v[m/min])$

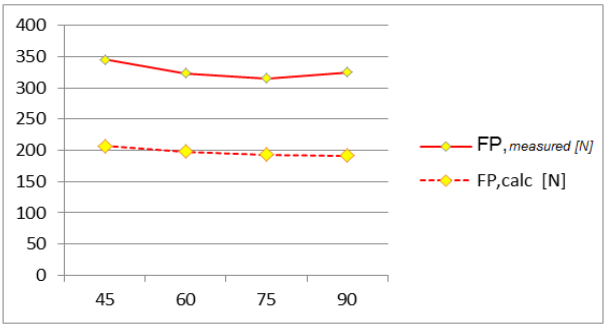

Fig. 4j The graph $F_P = f(\chi_r[°])$

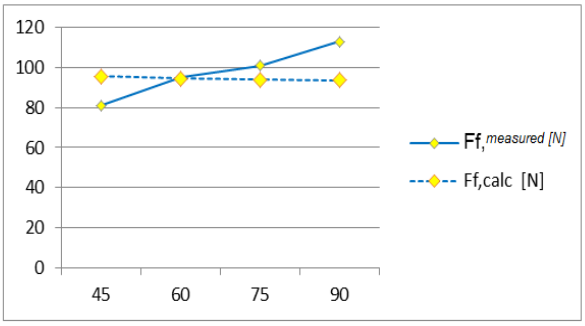

Fig. 4k The graph $F_f = f(\chi_r[°])$

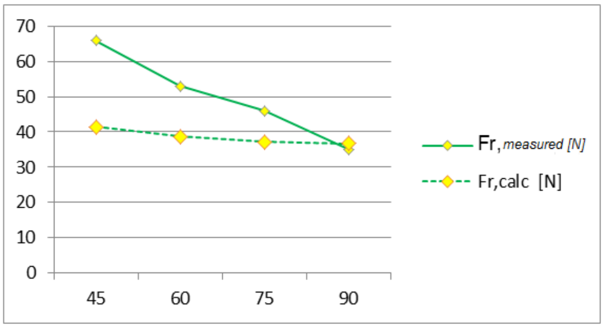

Fig. 4l The graph $F_r = f(\chi_r[°])$

Fig.4 The evolution of the turning force components depending on *f; t; v and* χ_r

The experimental cutting of aluminum (shown in table) has helped to draw the diagrams presented in this paper and by means of them to establish the following conclusions:

- The measured values were compared with those calculated of the resultant cutting forces, observing that the differences are small.
- There were plotted $F_{P,f,r} = f(f)$; $F_{P,f,r} = f(t)$; $F_{P,f,r} = f(v)$; $F_{P,f,r} = f(\chi_r)$ and the results were interpreted.
- Increasing the feed rate and the depth of cut lead to an increase the turning force components, cutting depth having more influence (the gradient of the line is higher with increasing of depth of cut)
- Increase the cutting speed leads to lower turning force components by reducing the resistance at higher temperatures of the workpiece
- The evolution of the feed rate component of cutting force ***Ff*** and of the passive component ***Fr*** in relation to the cutting edge angle is the consequence of geometrical position of the cutting edge to the direction of feed: if ***kr*** increases, ***Ff*** increases and decreases ***Fr***.
- The coefficients K_P, $k_{P1,1}$, p (respectively K_f, $k_{f1,1}$, f, K_r, $k_{r1,1}$, r) shall be determined experimentally and are valid for all operations for the constant thickness of chip, according to the same tool geometry, to the same speed and to the same materials for the workpiece and to the same tool equipment;
- To calculate the forces in other conditions should be used correction coefficients

6 REFERENCES

► **Deteşan, O.A., Vahnovanu, A.D.,** *The Dynamic Model of RTTRR Serial Robot – Iterations Outwards and Inwards the Robot's Mechanical Structure,* Acta Technica Napocensis, vol. 59, nr. 1, p. 25 - 32, Cluj-Napoca, 2016, ISSN 1221-5872

► **Deteşan, O.A.,** *The Dynamic Model of RTTRR Serial Robot – The Determination of the Generalized Driving Forces*, Acta Technica Napocensis, vol. 59, nr. 1, p. 33 - 38, Cluj-Napoca, 2016, ISSN 1221-5872

► **Deteşan, O.A.**, *The Path Planning of Industrial Robots Using Polynomial Interpolation, with Applications to Fanuc LR-Mate 100iB,* Acta Technica Napocensis, nr. 56, vol. IV, p. 665-670, Cluj-Napoca, 2013, ISSN 1221-5872.

► **Nedezki, Claudiu,** Julean Dănuț, *Bazele generării suprafeţelor: îndrumător de lucrări,* Edit. U.T.PRESS, 2008, ISBN 978-973-662-402-5, 147 pag.

► **Smith, Graham T.**, *"Cutting Tool Technology. Industrial Handbook"*, Springer-Verlag London Limited 2008.